ACS OMEGA

Open Access

http://pubs.acs.org/journal/acsodf

Article

Frankincense-Based Functionalized Multiwalled Carbon Nanotubes with Iron Oxide Composites for Efficient Removal of Crystal Violet: Kinetic and Equilibrium Analysis

Mushtaq Hussain, Syed Sulaiman Hussaini, Mohammad Shariq,* Najla AlMasoud, Ghadah Abdulrahman AlZaidy, Khaled F. Hassan, Syed Kashif Ali, Rehab E. Azooz, Mohd Asim Siddiqui, and Kondaiah Seku

Cite This: *ACS Omega* 2024, 9, 11459−11470

Read Online

ACCESS | Metrics & More | Article Recommendations | Supporting Information

ABSTRACT: In this study, novel adsorbents were developed by functionalizing multiwalled carbon nanotubes with frankincense (Fr-fMWCNT) and adding iron oxide (Fe_3O_4) to the adsorbent (Fr-fMWCNT-Fe_3O_4). The morphology, surface characteristics, and chemical nature of the synthesized samples were analyzed by using various characterization techniques. The prepared adsorbents were then applied for the elimination of the toxic dye, crystal violet (CV), from water-based solutions by employing a batch adsorption method. The effectiveness of materials for the adsorption of CV was investigated by tuning various effective experimental parameters (adsorbent dosage, dye quantity, pH, and contact time). In order to derive adsorption isotherms, the Langmuir and Freundlich adsorption models were investigated and compared. The Fr-fMWCNT and Fr-fMWCNT-Fe_3O_4 were found to remove 85 and 95% of the CV dye within 30 min of the adsorption experiment at pH 6, respectively. It was found that a pseudo-second-order reaction rate was consistent with the experimental adsorption kinetics. The equilibrium data demonstrated that the Langmuir model adequately explained the adsorption behavior of the CV dye on the Fr-fMWCNT and Fr-fMWCNT-Fe_3O_4 surfaces, respectively. According to the Langmuir study, the highest adsorption capacities of the dye are 434 mg/g for Fr-fMWCNT and 500 mg/g for Fr-fMWCNT-Fe_3O_4. Remediation of the CV dye using our novel composite materials has not been reported previously in the literature. The synthesized Fr-fMWCNT and Fr-fMWCNT-Fe_3O_4 adsorbents can be economical and green materials for the adsorptive elimination of CV dye from wastewater.

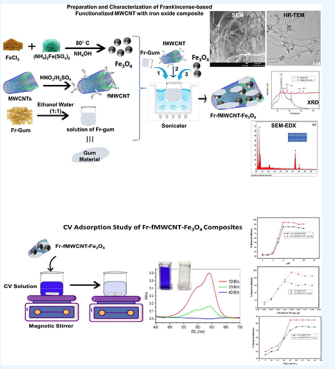

1. INTRODUCTION

Water is essential for drinking, agriculture, cleanliness, industry, and energy. However, excessive harvesting and population growth have increased the risk of freshwater resource extinction. The rampant discharge of effluent from various industries containing synthetic dyes, such as textiles, paper, and paint, has led to significant environmental concerns in recent years.[1,2] Every year, approximately 10,000 pigments and dyes are manufactured worldwide.[3,4] Dyes, in contrast to most organic substances, can gather visible spectrum light because they have a conjugated structure.[5−7] Removing color from dye-bearing wastewater is a challenging issue since it is difficult to treat with traditional techniques.[8,9] Textile industry effluents contain harmful chemicals and dyes that can negatively impact the environment and human health.[10−13] Therefore, finding effective treatment methods is crucial for decreasing the negative effects of industrial waste production on the environment. Crystal violet (CV), a synthetic cationic dye, has extensive uses in the physical and biological sciences. It belongs to the family of triphenylmethanes.[14,15] However, the carcinogenic nature of this dye and its ability to cause skin and digestive tract irritation have highlighted the need to address the issue of its environmental discharge.[16] Furthermore, CV's resistance to biodegradation means it can persist in the environment, posing a long-term threat to ecological systems.[17]

In the treatment of effluent-containing synthetic dyes, various biological, chemical, and physical methods (such as photocatalysis, flocculation, coagulation, reverse osmosis, and adsorption) can be employed.[18] Advanced oxidation processes and photocatalysis work together to use hydroxyl radicals ($OH^{\cdot}$) under mild conditions to remove pollutants from water. Heterogeneous photocatalysis can effectively degrade pollutants into water and CO_2 using UV, visible, or solar light with oxygen as the sole oxidant.[19] Researchers found that the chemically coprecipitated composite, which is made up of 60% g-C_3N_4 and 5% Cr-ZnO, can absorb more solar energy than

Received: October 13, 2023
Revised: February 12, 2024
Accepted: February 13, 2024
Published: February 28, 2024

ZnO, g-C_3N_4, and the g-C_3N_4/ZnO composite. As a result, it exhibited an impressive 93% degradation of methylene blue dye within 90 min through photocatalytic degradation.[20] Oxidative dye degradation refers to the breakdown of macromolecules and dyes caused by the influence of oxygen on the substrate, which leads to oxidation. This process gives rise to free radicals, which then interact with oxygen to form oxy- and peroxy-radicals.[21] In a study, Zhang et al. examined the oxidation process of different dyes using alkaline-activated peroxymonosulfate (PMS). The results showed that PMS successfully removed various dyes (including MB, orange G, and direct blue) under slightly alkaline conditions. The study determined that the sulfate radicals were the primary oxidizing agents accountable for the efficient degradation of colors in the alkaline-activated PMS system.[22] Although these methods effectively remove organic and inorganic pollutants, they are time-consuming, expensive, require many disposals, and frequently fail to remove resistant chemicals.[23,24] Adsorption, however, has proven to be the most adaptable and useful technology for removing dyes from effluent. It has consistently demonstrated excellent results in terms of its ability to remove dyes from effluents, making it the preferred choice for many industrial treatment processes.[25,26] Its versatility, cost-effectiveness, and wide applicability have also contributed to its popularity in the field of effluent treatment.[27] For the adsorptive elimination of dyes in wastewater, a variety of adsorbents and biosorbents have been used, including chitosan nanoparticles, modified montmorillonite, palm kernel shell-based activated carbon, and magnetic graphene oxide.[28−31]

Adsorbents are commonly derived from various sources, such as agricultural and industrial waste, biomass, clay, and carbonous materials. Natural zeolite was utilized by Maleha et al. to remove CV dye. Most of the dye was removed at room temperature at basic pH (pH = 10). Natural zeolite exhibited a maximal dye adsorption of 177.75 mg/g as compared to 84.11 mg/g adsorption for Merck-activated carbon.[32] Similarly, a bentonite-alginate composite was created using microwave heating and varying amounts of Na-alginate and bentonite. The composite was then utilized for the adsorption-based elimination of CV dye at 30, 50, and 70 °C in batch mode. The composite with the largest percentage of bentonite mass was determined to have the best adsorption capability.[33] Santosh et al. described the utilization of spirulina in the green production of iron oxide nanoparticles. Subsequently, they modified using ultrasonic waves, leading to an efficient adsorbent for cationic CV dye removal. So, with remarkable efficiency, the adsorbent was successful in removing CV dye. The ability of nanoparticles to decolorize CV dye from the solution was established using some analytical tools.[34] Carbon-based materials have been applied as adsorbents for the elimination of organic dyes due to their chemical stability and porous morphology. The utilization of carbon nanotubes to adsorb pollutants from effluents has been extensively investigated by researchers. Specifically, multiwalled carbon nanotubes (MWCNTs) have been employed by numerous scholars for the elimination of dyes, as evidenced by various studies.[35−38] MWCNTs are a promising carbon-based material for adsorption due to their excellent mechanical strength and high surface area. These can be modified with various materials, such as metal oxides, to enhance their adsorption capacity.[39] Iron oxide (FeO_x) is commonly used as a metal oxide modifier due to its good magnetic and adsorption properties.[40] Pourzamani et al. reported the creation of the MWCNTs-Fe_3O_4 nanocomposite and its application in eliminating diclofenac sodium. The nanocomposite showed high adsorption capacity for diclofenac sodium and reusability due to its magnetic nature.[41] The successful removal of ionic dyes by the MWCNTs/Fe_3O_4/PANI composite has been reported by Zhao. The composite exhibited excellent adsorption toward methyl orange and cango red.[42] Toxic heavy metal Hg (II) was removed via adsorption using a MWCNTs-Fe_3O_4 nanocomposite. Sadegh et al. determined using the Langmuir model that the nanocomposite had a good adsorption ability (238.78 mg g^{-1}).[43] CV dye was quickly and effectively removed from water solutions using activated carbon and magnetic iron oxide adsorbents. The various parameters, including thermodynamic factors affecting adsorption processes, were also examined.[44]

The adsorption ability of the MWCNTs can be further enhanced by modifying them with some natural resinous material. In this investigation, we demonstrate the elimination of CV dye using frankincense-based functionalized MWCNTs incorporating iron oxide, denoted as Fr-fMWCNT-Fe_3O_4. The existing literature does not appear to address the utilization of frankincense-based functionalized multiwalled carbon with iron oxide as an adsorbent for removing organic dyes, specifically CV. Frankincense, an aromatic resin derived from Boswellia trees, contains several biologically active compounds that exhibit antibacterial and antifungal properties.[45−47] In the context of adsorption, frankincense-based materials have demonstrated the potential to be effective adsorbents owing to their porous morphology and high surface area. Additionally, frankincense-based materials combined with other substances, such as iron oxide, can further enhance their selectivity for explicit pollutants and adsorption capacity. Despite the presence of several adsorbents in the field of dye remediation, researchers persist to search for better adsorbents with enhanced activity, specificity, and other parameters.[48]

Therefore, we proposed that using frankincense-based functionalized multiwalled carbon nanotubes (Fr-fMWCNT) and frankincense-based functionalized multiwalled carbon nanotubes with iron oxide (Fr-fMWCNT-Fe_3O_4) as an adsorbent for removing organic dyes, such as CV, could potentially offer several advantages over other conventional adsorbents, like lower cost, being more eco-friendly, and being a natural and sustainable material. Moreover, our preparation method also involves the use of no harsh chemicals and an energy-efficient, eco-friendly approach, leading to a cost-effective wastewater treatment solution.

2. MATERIALS AND METHODS

2.1. Materials. The MWCNT (purity: 99%, internal diameter: 5−10 nm, outer diameter: 10−30 nm, length: >10 μm, CNT content: 95−99%, surface area: 110−350 m^2/g) was obtained from Adnano Technologies Private Limited, India. These were chemically modified and then used as adsorbents for the elimination of dyes. The frankincense gum (100%) utilized in this work was of the Hojari kind and was procured from a nearby marketplace (Gurgaon, Haryana, India). The chemical formula of the components of frankincense has been provided in Supporting Information. While nitric acid and CV were bought from Merck, HC) and NaOH with a concentration of 98% was procured from SD Fine Chemical, a supplier based in India. Sulfuric acid (H_2SO_4, 98%) and nitric acid (HNO_3, 71%) were bought from Thomas Baker, a chemical supplier based in India.

https://doi.org/10.1021/acsomega.3c08011
ACS Omega 2024, 9, 11459−11470

2.2. Methods. *2.2.1. Modification of MWCNTs and Synthesis of Fr-fMWCNTs-Fe_3O_4.* The acid reflux method was used for functionalization of MWCNTs, as reported by Jeon et al. and Chen et al.[49,50] To prepare the Fr-fMWCNT-Fe_3O_4 composite, 0.4 g of frankincense gum was dispersed in an ethanol−water mixture, filtered to remove any suspended impurities, and mixed with 1.0 g of fMWCNT by sonication and stirring. The resulting composite was then washed, filtered, and dried. Next, the composite was coupled with magnetic Fe_3O_4-nanoparticles using a coprecipitation method described by Gharibshahi et al.[51] The resulting Fr-fMWCNT-Fe_3O_4 composite was washed with water and dried. The yield of the composite obtained was 1.2 g (80%, the yield was calculated based on FMWCNT and Fe_3O_4), and it was characterized using FTIR SEM, EDX, XRD, and HRTEM spectroscopy.

2.2.2. Dye Solution Preparation. The CV dye was dissolved in distilled water to produce a stock solution, which was then diluted to produce working solutions ranging from 20 to 120 mg/L. A UV−visible spectrophotometer (Hitachi-2800) was utilized to find the absorbance of these solutions at λ_{max} = 580 nm.

2.2.3. Adsorption Experiment. The study employed a 50 mL working volume of dye solution with diverse dilutions (20, 40, 60, 80, 100, and 120 mg/L) for batch adsorption experiments. The adsorbent dosages from 0.01 to 0.05 g/L at pH values of 2, 3, 6, 7, 8, and 10 were tested. The residual CV concentration was measured every 5 min at λ_{max} = 580 until equilibrium was reached. At equilibrium, eqs 1 and 2 were used to determine the % dye elimination and the quantity of dye adsorbed/unit mass of adsorbent (mg/g).

$$\text{Percentage removal}(\%) = [(C_i - C_t)/C_i] \times 100 \quad (1)$$

$$\text{Adsorption capacity}(\text{mg/g}) = [(C_i - C_e) \times V]/m \quad (2)$$

The variables C_i (mg/L), C_t (mg/L), and C_e (mg/L) represent the concentrations of the dye at the initial time, time t, and equilibrium, respectively. V (L) stands for the dye solution's volume, while m (g) stands for the adsorbent's mass. The study of the adsorption isotherm was conducted by employing the Langmuir and Freundlich adsorption isotherm models. Additionally, both the pseudo-first-order (PFO) and pseudo-second-order (PSO) models were utilized for the investigation of the adsorption kinetics.[52]

3. RESULTS AND DISCUSSION

3.1. Characterization of Fr-fMWCNT and Fr-fMWCNT-Fe_3O_4. FTIR is an essential method for doing functional group analysis.[47,53] The FTIR of the various samples was performed to confirm the existence of the corresponding functional groups (Figure 1). The peaks at 2406.10, 2373.86, 2156.37, 2162.37, 2071.07, 2028.31, and 1971.24 cm^{-1}, 1964.11 cm^{-1} are likely due to the stretching vibrations of C≡C, C≡N, C≡O, C═C, and C−C bonds which are present in both Fr-fMWCNT and Fr-fMWCNT-Fe_3O_4 samples due to carbon nanotubes, Boswellic acid derivatives, and some terpenes found in frankincense gum.[54−56] The peak at 1006 cm^{-1} is likely associated with the C−O bond stretching vibration, which is present in Boswellic acid derivatives and some terpenes found in frankincense gum.[57] The peaks appearing at 3400−3500 cm^{-1} are due to the moisture.

The observed peak at 766 cm^{-1} can be attributed to the Fe−O stretching vibrations of the Fe_3O_4 nanoparticles, suggesting the presence of Fe_3O_4 on the surface of the carbon nanotubes.[58] Based on the FTIR peaks, it appears that both composites contain functional groups associated with carbon−carbon and carbon−nitrogen triple bonds, carbon−oxygen double bonds, and various organic functional groups. In addition, the composite containing iron oxide also exhibits a peak associated with Fe−O bonds.[59]

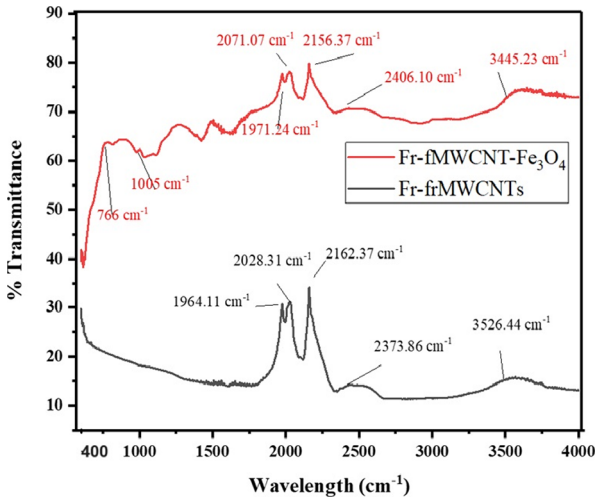

Figure 1. FTIR spectra of Fr-fMWCNT and Fr-fMWCNT-Fe_3O_4.

The SEM images of Fr-fMWCNT showed that the frankincense coating was well-distributed on the surface of the fMWCNT, which led to an improvement in the dispersion of the nanotube in a polymer matrix (Figure 2). SEM images of Fe_3O_4-coated frankincense-based MWCNTs (Fr-fMWCNTs-Fe_3O_4) revealed the uniformity of the Fe_3O_4 coating on the surface of the nanotubes as well as the overall structure of the nanocomposite. The images also show the uniform dispersion of the Fe_3O_4 and MWCNTs polymer matrices.

The EDX analysis of frankincense multiwalled carbon nanotubes Fr-fMWCNT, as shown in Figure 3a, indicates that these nanotubes are primarily composed of carbon (C) and oxygen (O). MWCNTs are cylindrical tubes made of multiple layers of graphene sheets rolled into a tube-like structure. The high carbon content observed in the EDX analysis is consistent with the expected composition of the MWCNTs. The presence of oxygen in the nanotubes can be attributed to the residual functional groups containing oxygen that are found on their surface. The EDX analysis of Fr-fMWCNT-Fe_3O_4 indicates the appearance of three elements: carbon (C), oxygen (O), and iron (Fe). The weight percentage of C and O indicates (Figure 3b) that "C" is the highest percentage element present in the sample, accounting for 25.98% of the total weight. The weight percentages of O and Fe indicate that oxygen is also present in the sample, accounting for 13.58% of the total weight. The weight percentage of Fe and O is the highest among the three elements, accounting for 60.44% of the total weight. This suggests that Fe_3O_4 is the dominant component in the sample. Fe_3O_4 is a compound of iron (Fe) and oxygen (O), also known as magnetite. Finally, the EDX analysis of multiwalled carbon with Fe_3O_4 revealed the existence of "C", "O", and "Fe", with Fe_3O_4 being the dominant component.

In the case of frankincense-based MWCNTs (Figure 4a) and their composites with iron oxide, the TEM images helped to reveal the dimension and distribution of the Fe_3O_4 nano-

https://doi.org/10.1021/acsomega.3c08011
ACS Omega 2024, 9, 11459−11470

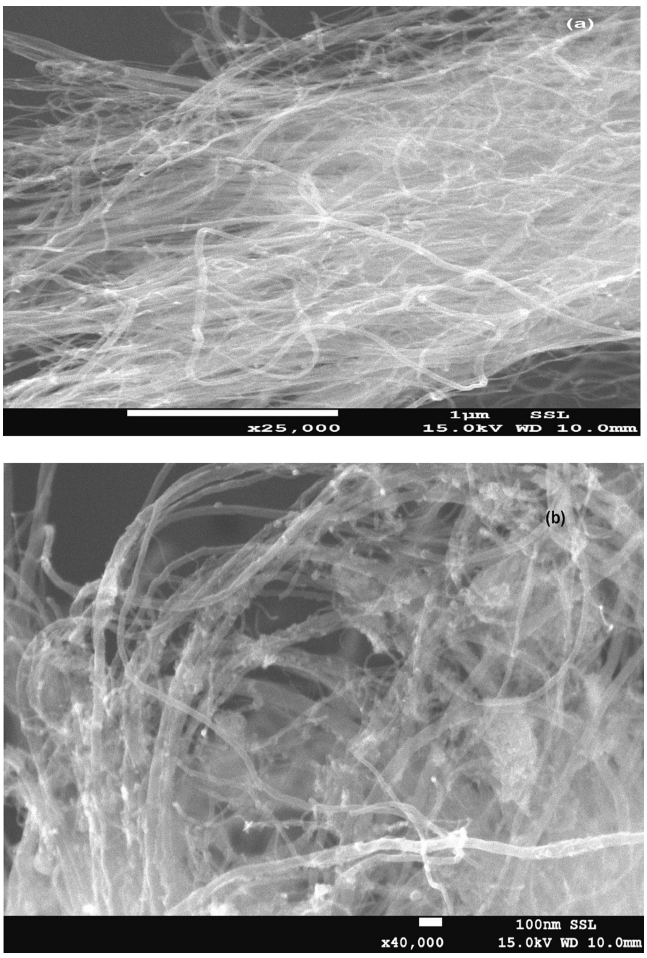

Figure 2. SEM image of (a) Fr-fMWCNT and (b) Fr-fMWCNT-Fe_3O_4.

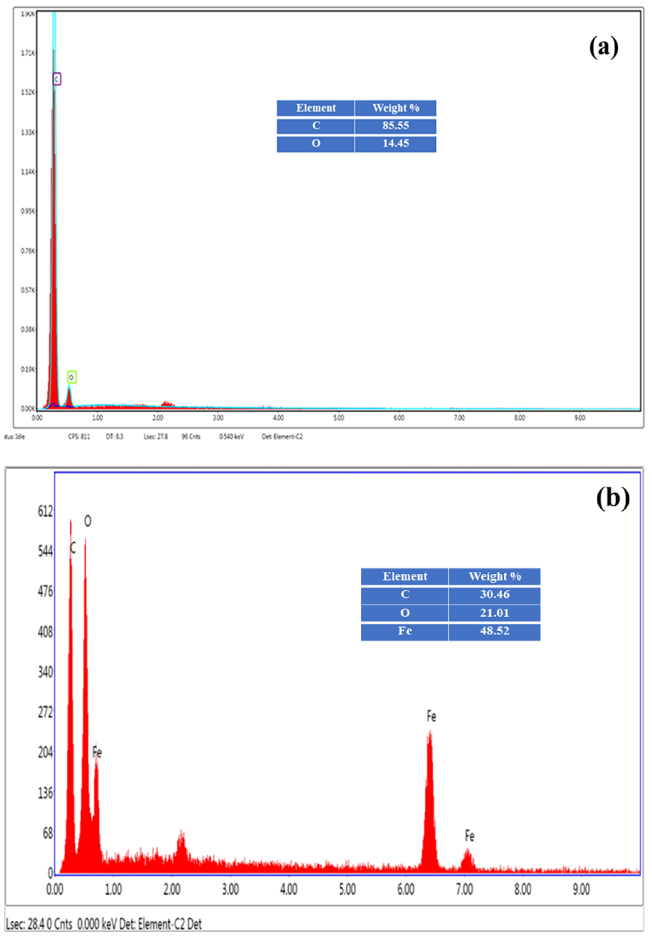

Figure 3. EDS of (a) Fr-fMWCNT and (b) Fr-fMWCNT-Fe_3O_4 composite.

particles on the carbon nanotube surface (Figure 4b). The observed size of the Fe_3O_4 nanoparticles in TEM images ranges between 11 and 15 nm. The uniform distribution and size of the iron oxide nanoparticles can affect the properties of the composite material, such as its magnetic and catalytic behavior. Furthermore, the addition of iron oxide nanoparticles to carbon nanotubes can enhance their properties, such as thermal conductivity, mechanical strength, and magnetic behavior.[43,60]

In summary, the TEM analysis of frankincense-based MWCNTs and frankincense-based MWCNTs with iron oxide composites can provide important insights into their structural properties, which can influence their functional properties. The reported diameter and interlayer spacing of the carbon nanotubes, as well as the size and distribution of the iron oxide nanoparticles, can affect the properties of the composite material.

Figure 5 shows the XRD pattern of Fr-fMWCNT-Fe_3O_4 in which peaks at 2θ values of 26.26° and 43.10°, which match the (002) and (110) planes of the MWCNT's structure (JCPDS No. 01−1061).[61] In the XRD of Fr-fMWCNT-Fe_3O_4, the MWCNTs exhibit faint diffraction peaks. This demonstrates that the composite material retains the original CNT structure.[62] The diffraction peaks seen at 2θ of 30.68°, 36.02°, 43.20°, 57.87°, and 63.38° may be ascribed to the existence of Fe_3O_4 nanoparticles (JCPDS No. 002−2321) inside the respective (202), (311), (400), (511), and (404) crystallographic planes of the Fe_3O_4 lattice. This demonstrates that the composite contains pure Fe_3O_4 nanoparticles without any contaminants.[63]

These two composites, Fr-fMWCNT and Fr-fMWCNT-Fe3O4 (Figure 6), both lost weight in the same way because they were made with the same gum material. Initial weight loss at 121.8 and 197.2 °C in Fr-fMWCNT and Fr-fMWCNT-Fe_3O_4, respectively, is due to the loss of oxygenated groups and water from the MWCNTs and from the gum surface. Further weight loss (425.5 °C) in Fr-fMWCNT and in Fr-fMWCNT-Fe_3O_4 (359.2 and 462.5 °C) could be ascribed to the degradation of the gum material on the surface of the MWCNTs particularly the removal of CO_2 and CO (due to degradation of COOH groups).[64] It could be clearly seen that the percentage of gum material in the Fr-fMWCNT-Fe_3O_4 composite is lower than the Fr-fMWCNT. Moreover, the Fr-fMWCNT-Fe_3O_4 composite shows greater thermal stability compared to the Fr-fMWCNT composite.[65]

3.2. Study of Various Factors on the Dye Adsorption by Fr-fMWCNT and Fr-fMWCNT-Fe_3O_4. *3.2.1. Effect of pH.* The impact of pH changes in dye on the adsorption effectiveness of produced samples was examined, and the findings are revealed in Figure 7. The outcomes in Figure 7 indicate that the Fr-fMWCNT-Fe_3O_4 nanocomposite displays superior performance compared to Fr-fMWCNT alone for pH values ranging from 2 to 12 in terms of removing cationic dyes.

https://doi.org/10.1021/acsomega.3c08011
ACS Omega 2024, 9, 11459−11470

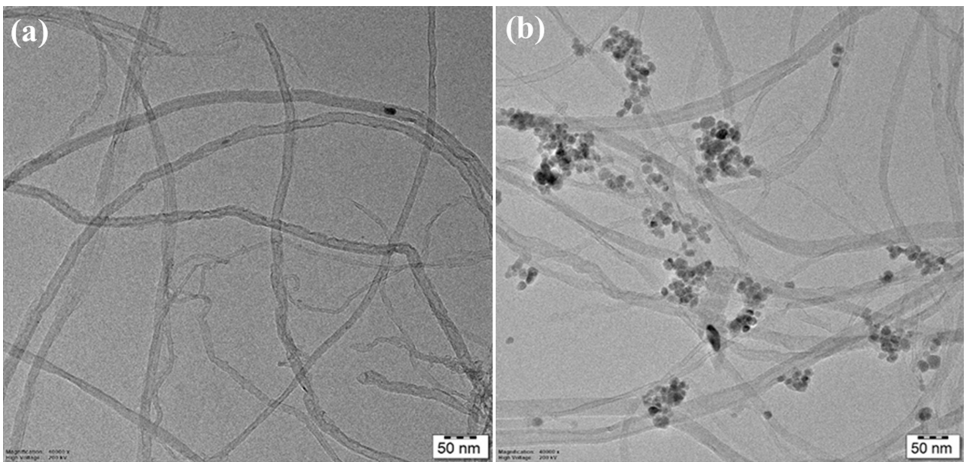

Figure 4. TEM images of (a) Fr-fMWCNT and (b) Fr-fMWCNT-Fe_3O_4.

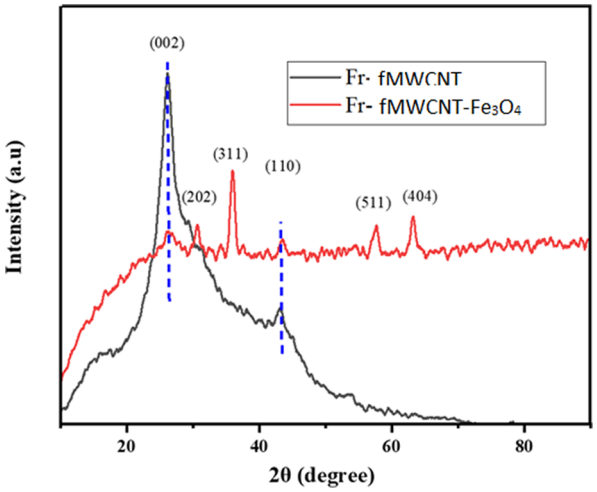

Figure 5. XRD pattern of Fr-MWCNT and the Fr-MWCNT-Fe_3O_4 composite.

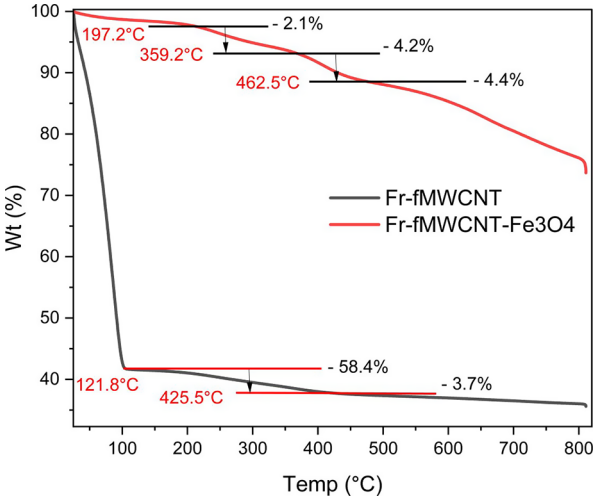

Figure 6. TGA study of Fr-fMWCNT and Fr-fMWCNT-Fe_3O_4 composite.

The optimal pH for removing CV dye with both Fr-fMWCNT and Fr-fMWCNT-Fe_3O_4 adsorbents is 6.

As the pH increases, both types of adsorbents demonstrate a rise in removal efficiency. The electrostatic attraction between

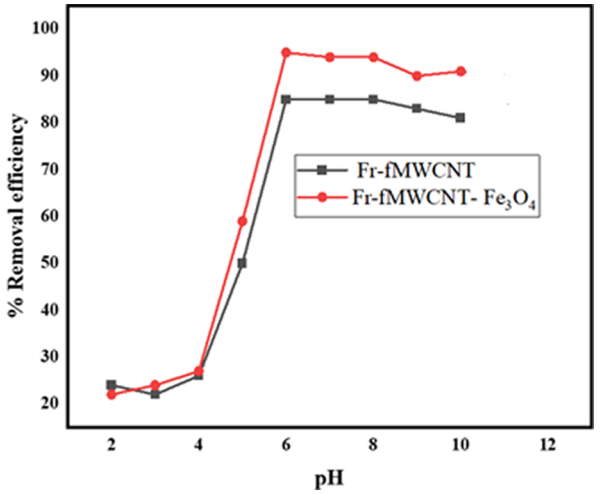

Figure 7. pH effect on dye adsorption by Fr-fMWCNT and Fr-fMWCNT-Fe_3O_4.

charged adsorbent surfaces and the cationic dye increases as the pH rises, indicating an increase in the removal efficiency for both adsorbents. However, the rate of adsorption exhibits a slower incline for pH values exceeding 7, suggesting that other adsorption mechanisms such as ion-exchange absorption, hydrogen bond, and $\pi-\pi$ interactions might supersede the electrostatic mechanism (Figure 7). This finding corroborates prior studies that have reported an improvement in cationic dye removal competence by using carbon-based adsorbents with an increase in pH. For instance, Wang et al. reported an optimal pH of 8.0 for removing malachite green dye with graphene oxide-based adsorbents, while Sulyman et al. found a pH of 6 to be optimal for removing CV dye with activated carbon-based adsorbents.[62,66,67] Moreover, at the active sites of the adsorbents, the OH group competes with the CV dye, leading to a decline in adsorption beyond a pH of 7.

In conclusion, the pH of the solution has a considerable impact on how well carbon-based adsorbents can absorb cationic dyes. Electrostatic contact is the main process that removes cationic dyes, and it becomes stronger as the pH rises. However, the slower adsorption rate increases for pH values higher than 7, suggesting the presence of additional adsorption mechanisms.[68]

https://doi.org/10.1021/acsomega.3c08011
ACS Omega 2024, 9, 11459−11470

3.2.2. Adsorbent Dosage Effect. Figure 8 shows the effect of different amounts of Fr-fMWCNT and Fr-fMWCNT-Fe_3O_4

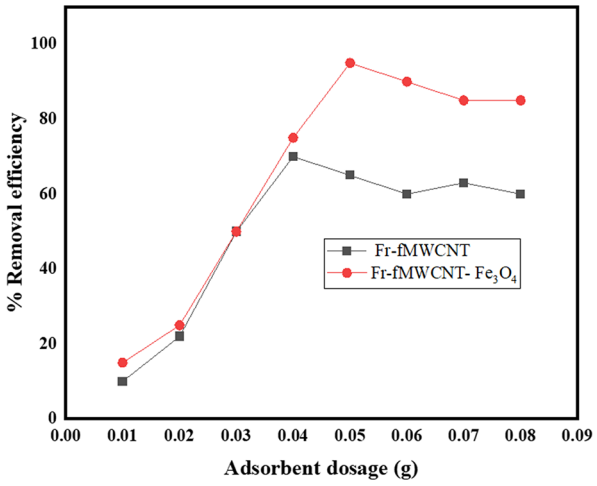

Figure 8. Variation of dye removal by changing the Fr-MWCNT and Fr-MWCNT-Fe_3O_4 dosages.

adsorbents on the removal of CV when the analyte concentration was 100 mg/L. Adsorbent dosages ranging from 0.01 to 0.08 g were utilized individually for this aim. The dye concentration dropped as the quantity of adsorbents increased. While the dosage of adsorbents increased, so did the number of accessible active sites and the removal efficiency of the studied dye. After looking at the test results, it was discovered that using 0.040 g of Fr-fMWCNT and 0.050 mg of Fr-fMWCNTs-Fe_3O_4 was the best way to remove the dye. No significant improvements were observed beyond these concentrations of the composites. Therefore, it was decided that 0.040 and 0.050 mg are the optimal concentrations for Fr-fMWCNT and Fr-fMWCNT-Fe_3O_4, respectively.

3.2.3. Effect of Contact Time. The term "contact time" pertains to the period during which the adsorbent and the target substance (in this case, CV) are in contact with each other. The findings indicate that with a rise in contact time, the removal efficiency of both adsorbents increases (Figure 9). When the contact time was 5 min, the removal efficiency of Fr-fMWCNT was 35%, while that of Fr-fMWCNT-Fe_3O_4 was 40%. However, as the contact time increased to 25 min, the removal efficiency of Fr-fMWCNT reached 70%, while that of Fr-fMWCNT-Fe_3O_4 increased to 85%. The improved removal efficiency with an increase in contact time can be attributed to the increased opportunity for the adsorbent to interact with the target substance, leading to more adsorption. At the initial contact time, only a small numbers of adsorption sites on the surface of the adsorbent were available for the target substance to interact with. However, as contact duration increased, more sites became available, resulting in higher removal efficiency.[69]

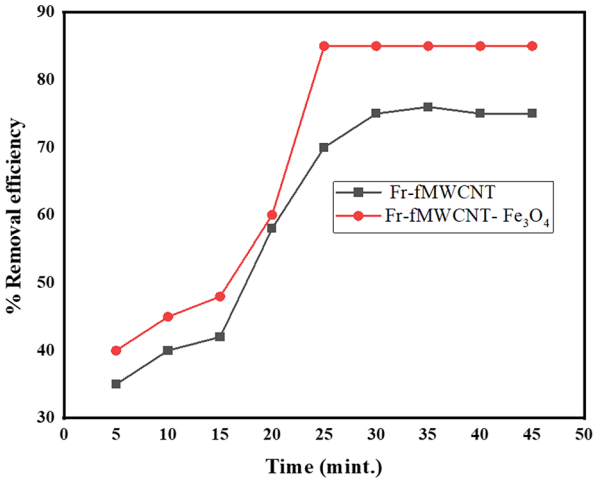

Figure 9. Change in dye removal by Fr-fMWCNT and Fr-fMWCNT-Fe_3O_4 with contact time variation.

After 25 min, the elimination efficiency of both adsorbents was found to be constant and then progressively returned to equilibrium. The study found that the optimal contact time for Fr-fMWCNT was 15 min, while that for Fr-fMWCNT-Fe_3O_4 was 20 min, after which no substantial variations in removal efficiency were found.

3.3. Adsorption Isotherm Study. Adsorption is a process of accumulating molecules or ions on the surface of a solid material from the liquid or gas phase. The study of adsorption isotherms provides crucial information about the adsorption mechanism, surface properties, and sorbent affinities. Three commonly used adsorption isotherm models are Freundlich's, Langmuir's, and Temkin's equations.[70] Freundlich's model is suitable for describing heterogeneous multilayer adsorption systems. The equation relates the K_F (L/mg) and adsorption intensity $(1/n)$ to the equilibrium concentration of the adsorbate (C_e) as follows:

$$\ln q_e = [1/n \times \ln C_e] + \ln K_F$$

where q_e is the equilibrium adsorbed quantity on the adsorbent (mg/g).

Langmuir's equation makes the assumption that there are only a small number of comparable adsorption sites on a uniformly distributed adsorbent surface. The equation relates the equilibrium concentration of the adsorbate (C_e) to the adsorbed amount (q_e, in mg/g) as follows:

$$1/q_e = [1/K_L \times q_{max}] + [1/q_{max} \times C_e]$$

The Langmuir constant, denoted as K_L, is a parameter that characterizes the adsorption capacity of a substance, measured in units of L/mg. q_{max} represents the maximum capacity of the adsorbent material.

UV−visible spectroscopy is commonly used to quantify and identify the amount of adsorbate in the liquid phase. The Langmuir and Freundlich adsorption models usually work in elucidating the adsorption characteristics of molecules onto a solid surface. According to the Langmuir model, adsorption happens at particular locations on the surface and once a site is occupied, no more adsorption can happen at that site. The Freundlich model shows that adsorption happens via a heterogeneous process, leading to the creation of several layers of adsorbate on the surface.

In the cases of Fr-fMWCNT and Fr-fMWCNT-Fe_3O_4, both the Langmuir and Freundlich models were utilized to examine the adsorption behavior of the molecules onto the carbon nanotubes with and without Fe_3O_4 nanoparticles. The Langmuir model reveals that the maximum adsorption capacity (Q_{max} = 500 mg/g) of Fr-fMWCNT-Fe_3O_4 (Figure 10a) is slightly more than that of Fr-fMWCNT (Q_{max} = 434 mg/g), which suggests that the Fe_3O_4 nanoparticles enhance the adsorption of the Fr-fMWCNT molecules onto the CNT

https://doi.org/10.1021/acsomega.3c08011
ACS Omega 2024, 9, 11459−11470

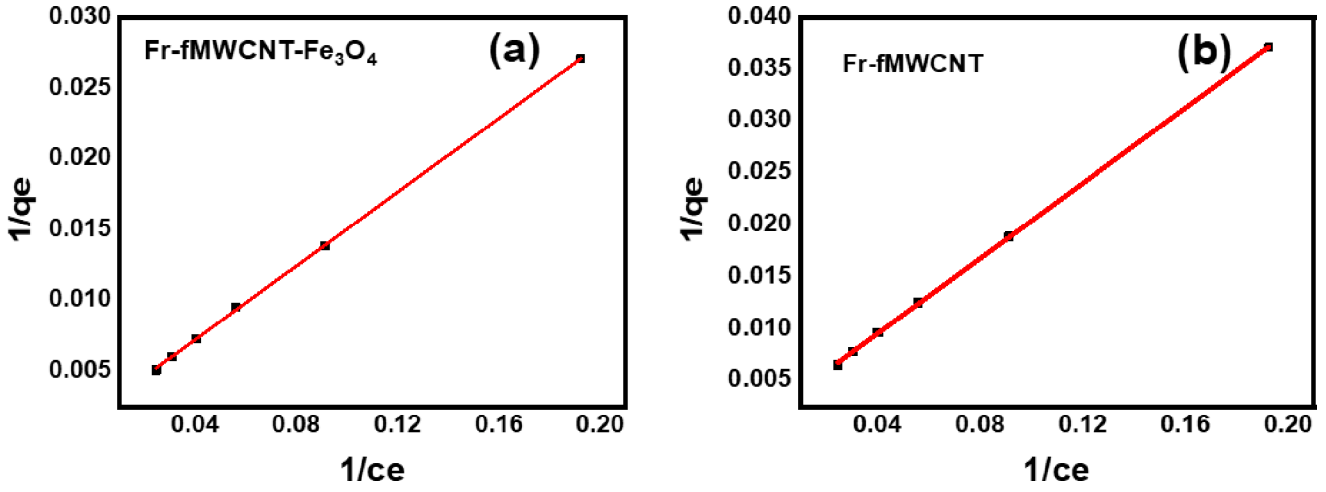

Figure 10. Langmuir adsorption isotherms for (a) Fr-fMWCNT-Fe_3O_4 and (b) Fr-fMWCNT.

(Figure 10b). The experimental data and projected values for both models exhibit a high degree of correlation (R^2), demonstrating a strong fit of the models to the data (Table 1).[71]

Table 1. Langmuir and Freundlich Adsorption for Fr-fMWCNT-Fe_3O_4 and Fr-fMWCNT

	Langmuir model		Fruendlich model		
adsorbent	Q_{max}	R^2	K_f	n	R^2
Fr-fMWCNT-Fe_3O_4	500	0.999	10.02	1.23	0.997
Fr-fMWCNT	434	0.998	4.89	1.08	0.998

The adsorption phenomenon of molecules onto carbon nanotubes may be explained well by using the Freundlich model. The surface's adsorption capacity is represented by the value of K_f, while the adsorption intensity is shown by the value of n. In this case, it is observed that the K_f of Fr-fMWCNT-Fe_3O_4 (Figure 11a) is higher than that of the Fr-fMWCNT (Figure 11b). However, the adsorption intensity (n) of Fr-fMWCNT-Fe_3O_4 is slightly higher than that of Fr-fMWCNT, representing that the existence of Fe_3O_4 may enhance the affinity of the carbon nanotube surface for Fr-fMWCNT molecules.[72]

To examine the correlation between the amount of adsorption and the equilibrium adsorption amount at a specific period, the PFO and PSO models were employed. The mathematical expression for the PFO model is as follows:

$$\log(q_e - q_t) = \log(q_e) - k_1 \times t/2.303$$

where q_e and q_t represent the equilibrium adsorption amounts and adsorption at different time (t), k_1 is the PFO rate constant, and 2.303 is the conversion factor for the natural logarithm to the logarithm with base 10.[73]

Similarly, the equation for the PSO model is

$$t/q_t = 1/(k_2 \times q_e^{\,2}) + t/q_e$$

where k_2 is the PSO rate constant.

The CV adsorption results, using two different adsorbents, Fr-fMWCNT and Fr-fMWCNT-Fe_3O_4 were evaluated using the PFO and PSO models, and then corresponding kinetic parameters were calculated.[74]

From Table 2, it can be observed that Fr-fMWCNT-Fe_3O_4 has a higher PFO rate constant (k_1) of −0.0001 min^{-1}, compared to Fr-fMWCNT with a k_1 value of −0.0006 min^{-1}. This suggests that the existence of Fe_3O_4 nanoparticles on the

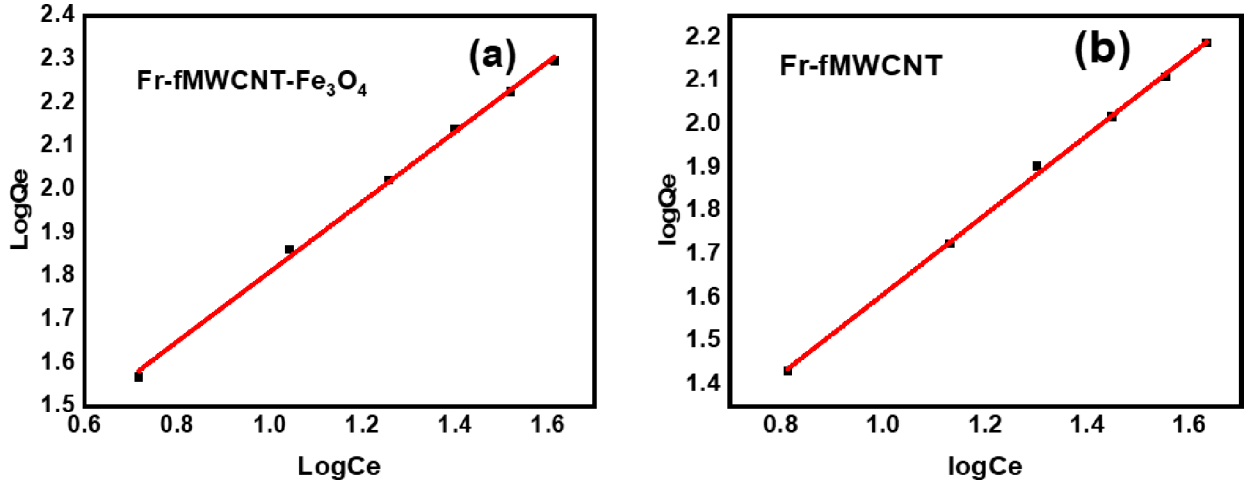

Figure 11. Freundlich adsorption isotherms for (a) Fr-fMWCNT-Fe_3O_4 and (b) Fr-fMWCNT.

https://doi.org/10.1021/acsomega.3c08011
ACS Omega 2024, 9, 11459−11470

Table 2. Kinetic Modeling Results

	pseudo-first-order			pseudo-second-order		
adsorbent	k_1	q_{e1}	R^2	k_2	q_{e2}	R^2
Fr-fMWCNT-Fe_3O_4	−0.0001	25.58	0.900	0.02	85.1	0.99982
Fr-fMWCNT	−0.0006	6.5	0.899	0.012	80.9	0.99991

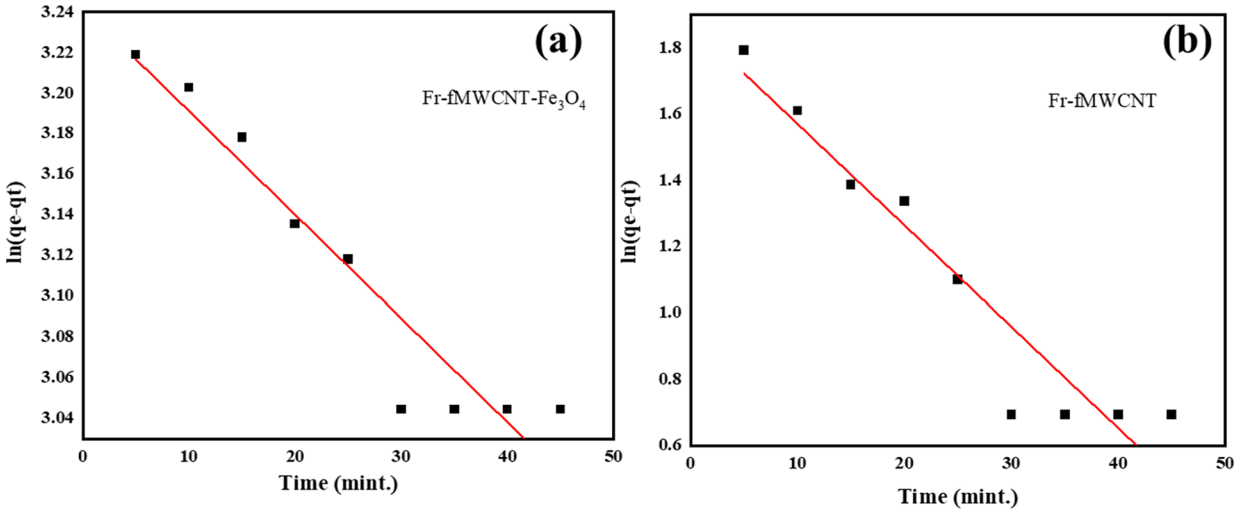

Figure 12. Pseudo-first-order reaction for (a) Fr-fMWCNT-Fe_3O_4 and (b) Fr-fMWCNT.

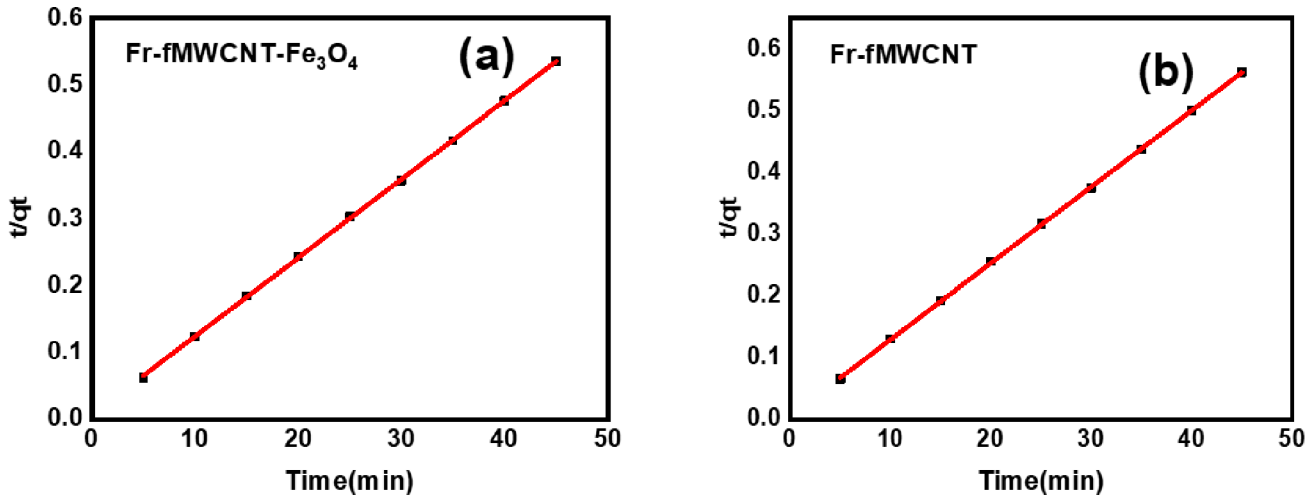

Figure 13. Pseudo-second-order reaction for (a) Fr-fMWCNT-Fe_3O_4 and (b) Fr-fMWCNT.

surface of the Fr-fMWCNT enhances the adsorption kinetics of CV (Figure 12a,b).

Similarly, the PSO rate constant (k_2) of Fr-fMWCNT-Fe_3O_4 is higher than that of Fr-fMWCNT representing that the adsorption of CV onto Fr-fMWCNT-Fe_3O_4 is more favorable and occurs at a rate faster than that onto Fr-fMWCNT.

The determination coefficient (R^2) for PSO models is high for both adsorbents, signifying that the data fit the PSO models well. The q_{e1} and q_{e2} values indicate the equilibrium adsorption capacity of each adsorbent, with Fr-fMWCNT-Fe_3O_4 showing a higher value than Fr-fMWCNT for both models (Figure 13a,b). These results are consistent with earlier research[75,76] which have shown that the incorporation of metal oxides onto carbon nanotubes can enhance their adsorption performance for various dyes and pollutants, including CV. Finally, the findings demonstrate that Fr-fMWCNT-Fe_3O_4 has a higher adsorption capacity and faster adsorption kinetics for CV than Fr-fMWCNT.

3.4. Mechanism of Adsorption. Earlier studies have pointed out several probable mechanisms for the adsorption of CV on the oxidized surface of MWCNTs.[77] Among them is $\pi-\pi$ interaction between the aromatic rings of the CV and the double bonds on the hexagonal structure of the carbon rings, which is likely possible with many adsorbents having exposed MWCNT surfaces.[78] However, in our study, there is gum material (with organic functional groups) covering the MWCNTs surface, as evidenced by the FTIR study showing functional groups (COOH/COOR) on the surface of MWCNTs. The other possible mechanism is the irreversible amidation reaction between the amino group of the CV and the carboxyl or lactonic groups of the adsorbents.[79] However, this mechanism is not possible because the amino group present in the CV is a tertiary group and the amidation

https://doi.org/10.1021/acsomega.3c08011
ACS Omega 2024, 9, 11459−11470

Table 3. Comparative Study of MWCNTs-Based Adsorbents for CV Elimination

composite	maximum adsorption capacity mg/g	time (min)	isotherm[a]	preparation method	references
MWCNTs and oxidized MWCNTs	37.17 and 42.1		L, F, T	hydrothermal	50
MWCNTs-montmorillonite clay	467.3	25	L, F	hydrothermal	80
microwave-synthesized MWCNT	2.6	25	L, F	microwave	81
$CoFe_2O_4$/MWCNTs and $ZnFe_2O_4$/MWCNTs	310.2	30	L, F, T	grafting by hydrothermal	82
alginate/poly(acrylamide)/carbon nanotubes			L, F	cross-linking by phase transfer method	83
L-tyrosine/MWCNTs	440	7	L, F, T	reaction of amino acids by chemical methods	84
hexachlorocyclotriphosphazene cross-linked sodium alginate/MWCNTs	662	25	L, F, B	catalytic methods for hydrogel preparation	85
sulfonic acid/MWCNTs	384	20	L, F, T	chemical methods	36
Gaur gum/MWCNTs	269	30	L	grafting methods	86
Fr-fMWCNT-Fe_3O_4 and Fr-fMWCNT	500 and 434	20 and 15	L, F	sonication	current study

[a]L = Langmuir; F = Freundlich; T = Temkin; B = BET isotherm.

reaction is not possible without hydrogen attached to the nitrogen group. Therefore, now the most probable mechanism is only $\pi-\pi$ interaction between the gum organic molecules and the aromatic ring of the CV.[50] Since the gum material is porous, it exposes more active sites for adsorption, leading to an enhancement in adsorption with temperature. At low value pH, the protons compete with CV for the active sites.

3.5. Comparative Study of Fr-fMWCNT and Fr-fMWCNT-Fe_3O_4 with Other MWCNT Adsorbents. Table 3 shows the removal capacities of other MWCNTs-based adsorbents for the adsorptive elimination of CV dye. It is evident that the surface-modified MWCNTs are more efficient with higher removal capacities due to their active functional groups. This is the main reason for continued research in the field for more efficient and specific adsorbents. Adsorbents (Fr-fMWCNT and Fr-fMWCNT-Fe_3O_4) in the current study show comparatively better removal capacities and a shorter time period as compared with other MWCNTs-based adsorbents. Moreover, the adsorbents are based on natural plant gum, which is a cheaply available, harmless, and eco-friendly material. In comparison, some of the other adsorbents mentioned in Table 3 were based on the functionalization of MWCNTs with heavy metals, proteins, or nondegradable polymers. Similar to earlier studies, the current study utilized Langmuir and Freundlich isotherm models.

4. CONCLUSIONS

In this investigation, researchers developed new adsorbents by adding frankincense to the MWCNT, with or without iron oxide (Fe_3O_4). The adsorbents' ability to remove CV dye from aqueous solutions was evaluated under various conditions, including pH and dye concentration. According to the investigation, the Langmuir model best described the data. The highest amounts of adsorption that Fr-fMWCNT-Fe_3O_4 and Fr-fMWCNT could hold were 500 and 434 mg/g, respectively. During the adsorption process at 25 °C, Fr-fMWCNT-Fe_3O_4 and magnetic Fr-fMWCNT performed best at a pH of 6, with optimum doses of 40 and 50 mg, respectively. The TGA clearly showed the high thermal stability of Fr-fMWCNT-Fe_3O_4 compared to the other composite. These findings suggest that Fr-fMWCNT-Fe_3O_4 could be an economical and eco-friendly material for eliminating organic pollutants from water-based solutions. The composites prepared are made from an economical and natural plant-based material that is used as a local medicine for various ailments in humans and animals. Therefore, it could be considered nontoxic and eco-friendly. Moreover, the process employed for the preparation of the composite materials is energy-efficient and rapid.

■ ASSOCIATED CONTENT

Supporting Information

The Supporting Information is available free of charge at https://pubs.acs.org/doi/10.1021/acsomega.3c08011.

Chemical formula of the components of frankincense; pH effect on the dye removal by Fr-fMMWCNT and Fr-fMMWCNT-Fe_3O_4; dye removal efficacy by changing Fr-fMWCNT and Fr-fMWCNT-Fe_3O_4 dosage; change in dye removal by the Fr-fMWCNT and Fr-fMWCNT-Fe_3O_4 with contact time variation; FTIR of frankincense gum; TGA of frankincense gum; DSC of frankincense gum; SEM-EDAX of frankincense gum; XRD of gum material; and SEM image of gum material (PDF)

■ AUTHOR INFORMATION

Corresponding Author

Mohammad Shariq − *Department of Physics, Faculty of Science, Integral University, Lucknow 226026, India;* orcid.org/0009-0001-9316-0008; Email: lucknow84iit@gmail.com

Authors

Mushtaq Hussain − *Engineering Department, College of Engineering and Technology, University of Technology and Applied Sciences, Shinas 324, Oman*

Syed Sulaiman Hussaini − *Engineering Department, College of Engineering and Technology, University of Technology and Applied Sciences, Shinas 324, Oman;* orcid.org/0000-0001-5191-7247

Najla AlMasoud − *Department of Chemistry, College of Science, Princess Nourah Bint Abdulrahman University, Riyadh 11671, Saudi Arabia*

Ghadah Abdulrahman AlZaidy − *Department of Physics, Faculty of Applied Science, Umm Al-Qura University, Makkah 24383, Saudi Arabia*

Khaled F. Hassan − *Department of Chemistry, College of Science, Jazan University, Jazan 45142, Saudi Arabia*

https://doi.org/10.1021/acsomega.3c08011
ACS Omega 2024, 9, 11459−11470

Syed Kashif Ali − *Department of Chemistry, College of Science, Jazan University, Jazan 45142, Saudi Arabia*
Rehab E. Azooz − *Department of Chemistry, College of Science, Jazan University, Jazan 45142, Saudi Arabia*
Mohd Asim Siddiqui − *Engineering Department, College of Engineering and Technology, University of Technology and Applied Sciences, Shinas 324, Oman*
Kondaiah Seku − *Engineering Department, College of Engineering and Technology, University of Technology and Applied Sciences, Shinas 324, Oman*

Complete contact information is available at:
https://pubs.acs.org/10.1021/acsomega.3c08011

Author Contributions

M.H.: original draft, funding acquisition, conceptualization; S.S.H.: investigation and methodology; M.S.: writing—review and editing; N.A.: review and editing; G.A.A.: review and editing; H.K.F.: validation and visualization; S.K.A.: resources and formal analysis; R.E.A.: formal analysis, review, and editing; M.A.S.: project administration and resources; K.S.: supervision and resources.

Notes

The authors declare no competing financial interest.

■ ACKNOWLEDGMENTS

The authors express their gratitude to the Ministry of Higher Education, Research, and Innovation (MoHERI), Sultanate of Oman, for the research grant (Research Grant No. BFP/RGP/EBR/21/225). This research work was supported by Princess Nourah bint Abdulrahman University Researchers Supporting Project number (PNURSP2024R18), Princess Nourah bint Abdulrahman University, Riyadh, Saudi Arabia.

■ REFERENCES

(1) Zahid, A. Synthesis of Mn-Doped ZnO Nanoparticles and Their Application in the Transesterification of Castor Oil. *Catalysts* **2023**, *13* (1), 105.
(2) Qamar, M. A.; et al. *Accelerated Decoloration of organic dyes from wastewater using ternary Metal/g-C3N4/ZnO nanocomposites: an investigation of impact of g-C3N4 concentration and Ni and Mn doping. Catalysts* **2022**, *12* (11), 1388.
(3) Sher, M.; et al. The controlled synthesis of gC 3 N 4/Cd-doped ZnO nanocomposites as potential photocatalysts for the disinfection and degradation of organic pollutants under visible light irradiation. *RSC Adv.* **2021**, *11* (4), 2025−2039.
(4) Haque, A.; et al. Degradation of reactive blue 19 dye using copper nanoparticles synthesized from Labeo rohita fish scales: a greener approach. *Polym. J. Environ. Stud* **2020**, *29* (1), 609−616.
(5) Lee, C.-P.; Li, C.-T.; Ho, K.-C. Use of organic materials in dye-sensitized solar cells. *Mater. Today* **2017**, *20* (5), 267−283.
(6) Hussain, M.; et al. Enhancing Cu^{2+} Ion Removal: An Innovative Approach Utilizing Modified Frankincense Gum Combined with Multiwalled Carbon Tubes and Iron Oxide Nanoparticles as Adsorbent. *Molecules* **2023**, *28* (11), 4494.
(7) Hussain, S.; et al. A facile low-cost scheme for highly photoactive Fe3O4-MWCNTs nanocomposite material for degradation of methylene blue. *Alexandria Engineering Journal* **2022**, *61* (11), 9107−9117.
(8) Javed, M.; et al. Integration of Mn-ZnFe2O4 with Sg-C3N4 for Boosting Spatial Charge Generation and Separation as an Efficient Photocatalyst. *Molecules* **2022**, *27* (20), 6925.
(9) Javed, M.; et al. Fabrication of Effective Co-SnO2/SGCN Photocatalysts for the Removal of Organic Pollutants and Pathogen Inactivation. *Crystals* **2023**, *13* (2), 163.
(10) Al-Mezeini, S. S. S.; et al. Design and Experimental Studies on a Single Slope Solar Still for Water Desalination. *Water* **2023**, *15* (4), 704.
(11) Iqbal, S.; et al. Designing highly potential photocatalytic comprising silver deposited ZnO NPs with sulfurized graphitic carbon nitride (Ag/ZnO/Sg-C3N4) ternary composite. *Journal of Environmental Chemical Engineering* **2021**, *9* (1), No. 104919.
(12) Qamar, M. A.; et al. Synthesis and applications of graphitic carbon nitride (g-C3N4) based membranes for wastewater treatment: A critical review. *Heliyon* **2023**, *9*, No. e12685.
(13) BaQais, A.; et al. NiO and magnetic CuFe2O4-based composite electrocatalyst for enhanced oxygen evolution reaction. *Eur. Phys. J. Plus* **2023**, *138*, 804.
(14) Alberoni, C.; et al. Ceria doping boosts methylene blue photodegradation in titania nanostructures. *Materials Chemistry Frontiers* **2021**, *5* (11), 4138−4152.
(15) Hafeez, M.; et al. Synthesis of cobalt and sulphur doped titanium dioxide photocatalysts for environmental applications. *Journal of King Saud University-Science* **2022**, *34* (4), No. 102028.
(16) Razzak, S. A.; et al. A comprehensive review on conventional and biological-driven heavy metals removal from industrial wastewater. *Environmental Advances* **2022**, *7*, No. 100168.
(17) Elgarahy, A.; et al. A critical review of biosorption of dyes, heavy metals and metalloids from wastewater as an efficient and green process. *Cleaner Engineering and Technology* **2021**, *4*, No. 100209.
(18) Sher, M.; et al. Synthesis of novel ternary hybrid g-C3N4@ Ag-ZnO nanocomposite with Z-scheme enhanced solar light-driven methylene blue degradation and antibacterial activities. *Journal of Environmental Chemical Engineering* **2021**, *9* (4), No. 105366.
(19) Asghar, A.; et al. Enhanced Electrochemical Performance of Hydrothermally Synthesized NiS/ZnS Composites as an Electrode for Super-Capacitors. *Journal of Cluster Science* **2022**, *33* (5), 2325−2335.
(20) Qamar, M. A.; et al. Highly efficient g-C3N4/Cr-ZnO nanocomposites with superior photocatalytic and antibacterial activity. *J. Photochem. Photobiol., A* **2020**, *401*, No. 112776.
(21) Chiam, S.-L.; et al. Highly efficient oxidative degradation of organic dyes by manganese dioxide nanoflowers. *Mater. Chem. Phys.* **2022**, *280*, No. 125848.
(22) Zhang, B.-T.; et al. Oxidation of dyes by alkaline-activated peroxymonosulfate. *J. Environ. Eng.* **2016**, *142* (4), No. 04016003.
(23) Etman, A. S.; et al. Facile water-based strategy for synthesizing MoO3−x nanosheets: efficient visible light photocatalysts for dye degradation. *ACS omega* **2018**, *3* (2), 2193−2201.
(24) Hussain, M. K.; Khalid, N. Surfactant-assisted synthesis of MoO3 nanorods and its application in photocatalytic degradation of different dyes in aqueous environment. *J. Mol. Liq.* **2022**, *346*, No. 117871.
(25) Quansah, J. O.; et al. Nascent rice husk as an adsorbent for removing cationic dyes from textile wastewater. *Applied Sciences* **2020**, *10* (10), 3437.
(26) Sun, P.; et al. Efficient removal of crystal violet using Fe3O4-coated biochar: the role of the Fe3O4 nanoparticles and modeling study their adsorption behavior. *Sci. Rep.* **2015**, *5* (1), 12638.
(27) Khairy, M.; Kamal, R.; Mousa, M. Anti-microbial and methylene blue dye adsorption properties of cotton fabrics modified with TiO2, Fe, Ag-doped TiO2, and graphene oxide nanomaterials. *Text. Res. J.* **2022**, *92* (17−18), 3299−3315.
(28) Benettayeb, A.; et al. Chitosan Nanoparticles as Potential Nano-Sorbent for Removal of Toxic Environmental Pollutants. *Nanomaterials* **2023**, *13* (3), 447.
(29) Nourouzi, M.; Chuah, T.; Choong, T. S. Equilibrium and kinetic study on reactive dyes adsorption by palm kernel shell-based activated carbon: in single and binary systems. *J. Environ. Eng.* **2009**, *135* (12), 1393−1398.
(30) Al Kausor, M.; et al. Montmorillonite and modified montmorillonite as adsorbents for removal of water soluble organic dyes: A review on current status of the art. *Inorg. Chem. Commun.* **2022**, *143*, No. 109686.

(31) Othman, N. H.; et al. Adsorption kinetics of methylene blue dyes onto magnetic graphene oxide. *Journal of Environmental Chemical Engineering* **2018**, *6* (2), 2803−2811.
(32) Sarabadan, M.; Bashiri, H.; Mousavi, S. M. Removal of crystal violet dye by an efficient and low cost adsorbent: Modeling, kinetic, equilibrium and thermodynamic studies. *Korean Journal of Chemical Engineering* **2019**, *36*, 1575−1586.
(33) Fabryanty, R.; et al. Removal of crystal violet dye by adsorption using bentonite−alginate composite. *Journal of Environmental Chemical Engineering* **2017**, *5* (6), 5677−5687.
(34) Bhukal, S.; et al. Spirulina Based Iron Oxide Nanoparticles for Adsorptive Removal of Crystal Violet Dye. *Top. Catal.* **2022**, *65*, 1675−1685.
(35) Sabna, V.; Thampi, S. G.; Chandrakaran, S. Adsorption of crystal violet onto functionalised multi-walled carbon nanotubes: equilibrium and kinetic studies. *Ecotoxicology and Environmental Safety* **2016**, *134*, 390−397.
(36) Mustafanejad, F.; et al. Efficient removal of crystal violet by sulphonic-modified multi-walled carbon nano-tube and graphene oxide. *Nanotechnol. Environ. Eng.* **2021**, *6* (2), 30.
(37) Sellaoui, L.; et al. Modeling the adsorption of divalent metallic cations onto multi-walled carbon nanotubes functionalized with COOH. *J. Mol. Liq.* **2022**, *366*, No. 120275.
(38) Adewoye, T.; et al. Optimization of the adsorption of total organic carbon from produced water using functionalized multi-walled carbon nanotubes. *Heliyon* **2021**, *7* (1), No. e05866.
(39) Egbosiuba, T. C.; et al. Adsorption of Cr (VI), Ni (II), Fe (II) and Cd (II) ions by KIAgNPs decorated MWCNTs in a batch and fixed bed process. *Sci. Rep.* **2021**, *11* (1), 75.
(40) Li, Y.; et al. Efficient removal of methyl blue from aqueous solution by using poly (4-vinylpyridine)−graphene oxide−Fe3O4 magnetic nanocomposites. *J. Mater. Sci.* **2019**, *54* (10), 7603−7616.
(41) Pourzamani, H.; Hajizadeh, Y.; Mengelizadeh, N. Application of three-dimensional electrofenton process using MWCNTs-Fe3O4 nanocomposite for removal of diclofenac. *Process Safety and Environmental Protection* **2018**, *119*, 271−284.
(42) Zhao, Y.; et al. Hierarchical MWCNTs/Fe3O4/PANI magnetic composite as adsorbent for methyl orange removal. *J. Colloid Interface Sci.* **2015**, *450*, 189−195.
(43) Sadegh, H.; et al. MWCNTs-Fe3O4 nanocomposite for Hg (II) high adsorption efficiency. *J. Mol. Liq.* **2018**, *258*, 345−353.
(44) Hamidzadeh, S.; Torabbeigi, M.; Shahtaheri, S. J. Removal of crystal violet from water by magnetically modified activated carbon and nanomagnetic iron oxide. *J. Environ. Health Sci. Eng.* **2015**, *13*, 8.
(45) Al-Yasiry, A. R. M.; Kiczorowska, B. Frankincense−therapeutic properties. *Advances in Hygiene and Experimental Medicine* **2016**, *70*, 380−391.
(46) Rashan, L.; et al. Boswellia gum resin and essential oils: potential health benefits− an evidence based review. *International Journal of Nutrition, Pharmacology, Neurological Diseases* **2019**, *9* (2), 53−71.
(47) Taqiullah, S. M.; et al.. Utilization of infrared, Raman spectroscopy for structural analysis of alkali boro-germanate glasses. *J. Taibah Univ. Sci.* **2022**, *16* (1), 820−827.
(48) Raninga, M.; et al. Modification of activated carbon-based adsorbent for removal of industrial dyes and heavy metals: A review. *Materials Today: Proceedings* **2023**, *77*, 286−294.
(49) Jeon, I.-Y.et al.Functionalization of carbon nanotubes. *Carbon nanotubes-polymer nanocomposites*, 2011, vol *6*; pp 91−110.
(50) Chen, L.; Xie, H.; Yu, W.Functionalization methods of carbon nanotubes and its applications. *Carbon nanotubes applications on electron devices*, 2011, vol *41*; pp 215−222.
(51) Gharibshahi, R.; et al. Hybridization of superparamagnetic Fe3O4 nanoparticles with MWCNTs and effect of surface modification on electromagnetic heating process efficiency: A microfluidics enhanced oil recovery study. *Fuel* **2020**, *282*, No. 118603.
(52) Li, Z.; et al. Adsorption of hazardous dyes on functionalized multiwalled carbon nanotubes in single and binary systems: Experimental study and physicochemical interpretation of the adsorption mechanism. *Chemical Engineering Journal* **2020**, *389*, No. 124467.
(53) Zaid, M.; et al. Comparative structural, optical, and dielectric studies of Zn1− x Mn x/2A x/2O (A= Ni, Co and x= 0.24) nanoparticles. *Appl. Phys. A: Mater. Sci. Process.* **2022**, *128* (11), 1002.
(54) Regert, M.; et al. Reconstructing ancient Yemeni commercial routes during the Middle Ages using structural characterization of terpenoid resins. *Archaeometry* **2008**, *50* (4), 668−695.
(55) Ma, P. C.; Kim, J.-K.; Tang, B. Z. Functionalization of carbon nanotubes using a silane coupling agent. *Carbon* **2006**, *44* (15), 3232−3238.
(56) Chiang, I.; et al. Purification and characterization of single-wall carbon nanotubes. *J. Phys. Chem. B* **2001**, *105* (6), 1157−1161.
(57) Fatimah, A.-O.; et al. Antifungal potential of aqueous extract of Boswellia carteri. *J. Pure Appl. Microbiol* **2019**, *13* (4), 2375−2381.
(58) Ananthi, S.; et al. Natural tannic acid (green tea) mediated synthesis of ethanol sensor based Fe3O4 nanoparticles: Investigation of structural, morphological, optical properties and colloidal stability for gas sensor application. *Sens. Actuators, B* **2022**, *352*, No. 131071.
(59) Rezazadeh, L.; et al. Synthesis and characterization of magnetic nanoparticles from raffinate of industrial copper solvent extraction plants. *Mater. Chem. Phys.* **2019**, *229*, 372−379.
(60) Sadegh, H.; Shahryari-ghoshekandi, R.; Kazemi, M. Study in synthesis and characterization of carbon nanotubes decorated by magnetic iron oxide nanoparticles. *International Nano Letters* **2014**, *4*, 129−135.
(61) Yao, C.; et al. Hierarchical Core−Shell Co2N/CoP Embedded in N, P-doped Carbon Nanotubes as Efficient Oxygen Reduction Reaction Catalysts for Zn-air Batteries. *Small* **2022**, *18* (20), No. 2108094.
(62) Wang, Z.; et al. The selective adsorption performance and mechanism of multiwall magnetic carbon nanotubes for heavy metals in wastewater. *Sci. Rep.* **2021**, *11* (1), 16878.
(63) Zhao, P.; et al. Removal of Cu (II) ions from aqueous solution by a magnetic multi-wall carbon nanotube adsorbent. *Chemical Engineering Journal Advances* **2021**, *8*, No. 100184.
(64) Tomova, A.; et al. Functionalization and characterization of MWCNT produced by different methods. *Acta Phys. Polym., A* **2016**, *129* (3), 405−408.
(65) Arunkumar, T.; et al. Synthesis and characterisation of multi-walled carbon nanotubes (MWCNTs). *International Journal of Ambient Energy* **2020**, *41* (4), 452−456.
(66) Wang, G.; et al. Acrylic acid functionalized graphene oxide: High-efficient removal of cationic dyes from wastewater and exploration on adsorption mechanism. *Chemosphere* **2020**, *261*, No. 127736.
(67) Sulyman, M.; et al. Development, characterization and evaluation of composite adsorbent for the adsorption of crystal violet from aqueous solution: Isotherm, kinetics, and thermodynamic studies. *Arabian Journal of Chemistry* **2021**, *14* (5), No. 103115.
(68) Madhavakrishnan, S.; et al. Adsorption of crystal violet dye from aqueous solution using Ricinus communis pericarp carbon as an adsorbent. *Journal of Chemistry* **2009**, *6*, 1109−1116.
(69) Bagotia, N.; Sharma, A. K.; Kumar, S. A review on modified sugarcane bagasse biosorbent for removal of dyes. *Chemosphere* **2021**, *268*, No. 129309.
(70) Muthukumaran, C.; Sivakumar, V. M.; Thirumarimurugan, M. Adsorption isotherms and kinetic studies of crystal violet dye removal from aqueous solution using surfactant modified magnetic nano-adsorbent. *Journal of the Taiwan Institute of Chemical Engineers* **2016**, *63*, 354−362.
(71) Yang, S.-T.; et al. Removal of methylene blue from aqueous solution by graphene oxide. *J. Colloid Interface Sci.* **2011**, *359* (1), 24−29.
(72) Abutaleb, A.; et al. Fe3O4-multiwalled carbon nanotubes-bentonite as adsorbent for removal of methylene blue from aqueous solutions. *Chemosphere* **2023**, *316*, No. 137824.

https://doi.org/10.1021/acsomega.3c08011
ACS Omega 2024, 9, 11459−11470

(73) Khodabandehloo, A.; Rahbar-Kelishami, A.; Shayesteh, H. Methylene blue removal using Salix babylonica (Weeping willow) leaves powder as a low-cost biosorbent in batch mode: Kinetic, equilibrium, and thermodynamic studies. *J. Mol. Liq.* **2017**, *244*, 540−548.
(74) AbdEl-Salam, A.; Ewais, H.; Basaleh, A. Silver nanoparticles immobilised on the activated carbon as efficient adsorbent for removal of crystal violet dye from aqueous solutions. A kinetic study. *J. Mol. Liq.* **2017**, *248*, 833−841.
(75) Sivashankar, R.; et al. Magnetic composite an environmental super adsorbent for dye sequestration−A review. *Environmental Nanotechnology, Monitoring & Management* **2014**, *1*, 36−49.
(76) Abdel-Raouf, M.E.-S.; et al. Optimization, Kinetics, and Isotherm Studies of Methyl Thioninium Chloride Removal from Simulated Solutions Using Chitosan Derivatives. *ACS omega* **2023**, *8* (37), 33580−33592.
(77) Lin, D.; Xing, B. Adsorption of phenolic compounds by carbon nanotubes: role of aromaticity and substitution of hydroxyl groups. *Environ. Sci. Technol.* **2008**, *42* (19), 7254−7259.
(78) Gotovac, S.; et al. Effect of nanoscale curvature of single-walled carbon nanotubes on adsorption of polycyclic aromatic hydrocarbons. *Nano Lett.* **2007**, *7* (3), 583−587.
(79) Wu, W.; et al. Influence of functional groups on desorption of organic compounds from carbon nanotubes into water: insight into desorption hysteresis. *Environ. Sci. Technol.* **2013**, *47* (15), 8373−8382.
(80) Puri, C.; et al. Optical absorption investigations for efficient crystal violet dye removal from wastewater via carbon nanotubes: Montmorillonite-based nanocomposite. *Luminescence* **2023**, *38* (7), 1257−1267.
(81) Qureshi, S. S.; et al. Microwave-assisted synthesis of carbon nanotubes for the removal of toxic cationic dyes from textile wastewater. *J. Mol. Liq.* **2022**, *356*, No. 119045.
(82) Martins, A.; Nunes, N. Adsorption of a textile dye on commercial activated carbon: A simple experiment to explore the role of surface chemistry and ionic strength. *J. Chem. Educ.* **2015**, *92* (1), 143−147.
(83) da Costa, J. S.; et al. Composite aerogels of alginate/poly (acrylamide)/carbon nanotubes with enhanced performance for cationic dyes adsorption. *Materials Science and Engineering: B* **2023**, *298*, No. 116820.
(84) Saxena, M.; Sharma, N.; Saxena, R. Highly efficient and rapid removal of a toxic dye: adsorption kinetics, isotherm, and mechanism studies on functionalized multiwalled carbon nanotubes. *Surfaces and Interfaces* **2020**, *21*, No. 100639.
(85) Hu, Z.-P.; et al. Preparation of the hexachlorocyclotriphosphazene crosslinked sodium alginate polymer/multi-walled carbon nanotubes composite powder for the removal of the cationic dyes. *J. Mol. Struct.* **2022**, *1262*, No. 133050.
(86) Simran, F.; et al. Removal of crystal violet dye using grafted guar gum along with nanoclay and MWCNT. *Advanced Materials Letters* **2022**, *13* (1), 2201−1686.

https://doi.org/10.1021/acsomega.3c08011
ACS Omega 2024, 9, 11459−11470